Wrinkles Individuality Preserving Aged Texture Generation using Multiple Expression Images

Pavel A. Savkin[1], Tsukasa Fukusato[2], Takuya Kato[1] and Shigeo Morishima[1]
[1]*Waseda University, Tokyo, Japan*
[2]*The University of Tokyo, Tokyo, Japan*

Keywords: Texture Synthesis, Facial Aging, Aged Wrinkles, And Facial Individuality.

Abstract: Aging of a human face is accompanied by visible changes such as sagging, spots, somberness, and wrinkles. Age progression techniques that estimate an aged facial image are required for long-term criminal or missing person investigations, and also in 3DCG facial animations. This paper focuses on aged facial texture and introduces a novel age progression method based on medical knowledge, which represents an aged wrinkles shapes and positions individuality. The effectiveness of the idea including expression wrinkles in aging facial image synthesis is confirmed through subjective evaluation.

1 INTRODUCTION

Facial aging is widely studied in computer vision fields. Age classification of input faces has been particularly well-studied and various methods have been proposed (Shu et al., 2016).

One of the well-known application for facial age progression is a criminal investigation. High-quality aged facial images would help camera-based authentication systems to find such criminals or missing person. Facial image can be aged with manual assistance by special artists having medical knowledge (age, 2011), but aging a facial image requires high-level skills and creating photorealistic aged facial images of each criminal and missing person worldwide is impractical. Therefore, creating aged facial images without special skills has been widely researched. Since it is recognized in the facial authentication field that authentication accuracy would be improved by also considering the skin texture [9], these age progression methods can be improved by providing additional individuality features such as wrinkles, spots, luster, and somberness.

Aging features undergo two major types of visible changes: surface skin changes such as spots, somberness, and wrinkles (Farage et al., 2008), and facial shape changes under sagging or gravity (Coleman and Grover, 2006). Facial wrinkles are among the most significant changes, especially in older people. Wrinkling is caused by internal factors (reduction in skin elasticity due to repetitive movements of facial muscles) and external factors (smoking and irradiation by direct sunlight) (Farage et al., 2008)(Piérard et al., 2003). Especially, internal factors of a single individual are invariant with age. Therefore, it is safe to say that wrinkling is one of the most important, immutable, and predictable changes in aging.

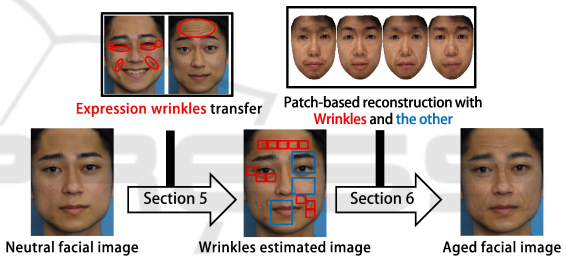

Figure 1: Workflow of our proposed method. First, by inspiring to the medical knowledge, expression wrinkles are transferred to provide a guideline for the aged face synthesis. Then, a patch-based synthesis approach is conducted to generate a wrinkles shape- and position-preserving aged facial image.

This paper focuses on aged facial texture and proposes an age progression method based on the medical knowledge (Piérard et al., 2003) that aged wrinkles emerge from the wrinkles appearing in the expressions of younger faces (define as expression wrinkles). To examine this assumption, we modify the texture synthesis method. With prepared multiple input facial images: one with a neutral expression (neutral facial image) and others with expression wrinkles (expression facial images), We transfer the expression wrinkles onto the neutral facial image, which can be treated as ”guide wrinkles” that indicates where to synthesize aged wrinkles. Using the wrinkles transferred image and a facial images database of the target

Savkin, P., Fukusato, T., Kato, T. and Morishima, S.
Wrinkles Individuality Preserving Aged Texture Generation using Multiple Expression Images.
DOI: 10.5220/0006614405490557
In *Proceedings of the 13th International Joint Conference on Computer Vision, Imaging and Computer Graphics Theory and Applications (VISIGRAPP 2018) - Volume 4: VISAPP*, pages 549-557
ISBN: 978-989-758-290-5

age, we represent the age-likeness in wrinkles, spots, and somberness by a patch-based texture reconstruction method. To analyze the effectiveness, we create a new database with standardized lighting, head pose, resolution, and races with only Japanese. The subjective evaluation improved by including the expression wrinkles in image synthesis under the created database, which suggests that the accuracy can be improved of other age progression methods.

2 RELATED WORK

2.1 Linear Combination and Neural Networks

Among the several methods for generating aged facial images (Shu et al., 2016), most researchers adopt linear combination models. Several methods based on active appearance models (AAMs) (Patterson et al., 2006)(Park et al., 2010)(Suo et al., 2010) have been proposed. For other methods, Scherbaum et al. (Scherbaum et al., 2007) reconstructed an aged face in three dimensions. The average face-based method that applies the features in average faces of different ages to the input facial image while accounting for skin color and the lighting environment were introduced by Kemelmacher et al. (Kemelmacher-Shlizerman et al., 2014). Shu et al. (Shu et al., 2015) and Yang et al. (Yang et al., 2016) proposed a linear combination-based method that preserves age-invariant individual features or trains age properties by Hidden Factor Analysis, respectively. The method of Wang et al.(Wang et al., 2016) and Zhang et al. (Zhang et al., 2017) proposed a method based on neural networks, which showed a better performance. These latest linear combination or neural network-based methods improve the cross-age face verification rate by considering the age-invariant features or by age-evolution-based training. However, the individuality can be further improved by considering individual skin features that are age-dependent, such as wrinkles, spots, luster, and somberness. Also, generating highly detailed aged facial images are common problems in both methods.

2.2 Texture Synthesis

Maejima et al. (Maejima et al., 2014) proposed an age progression method based on texture synthesis. They synthesized a statistical wrinkle pattern model to an input facial image and then applied a patch-based reconstruction method called Visiolization (Mohammed et al., 2009) by using a database of a target age. Finally, they synthesized the reconstructed image to the input facial image. During the reconstructed image synthesis, they excluded the eyes, nose, and mouth areas to maintain their individuality. While poorly defined edge textures in linear combination and neural network methods are problematic, Maejima et al. employed a reconstruction approach by using original textures in the database, rather than combining ones. In this method, accounting for the individuality in skin texture would also achieve a better accuracy.

2.3 Our Method

In all of the above methods, the authentication rate and visual plausibility of aged facial images can be improved by considering the aging-induced individuality in skin texture. Our main aim is to provide such a new features for incorporation into these methods in texture generation.

Based on medical knowledge and by allowing inputs to be multiple images, we assume that the shapes and positions of wrinkles are individually preserved in the age progression. To examine its effect correctly in terms of visual plausibleness, we consider two things. First, we modify the age progression method of Maejima et al. (Maejima et al., 2014), to obtain fine wrinkles in the aged face. Second, to improve the visual plausibility, we construct a completely new database with various ages, and with standardized lighting, head pose, and race with only Japanese. Fig. 1 shows the workflow of our proposed method. The shapes and positions of the aged wrinkles are estimated from the neutral and expression facial images. While reconstructing the image using the target-age database, the local (wrinkles) and global features (cheek luster etc.) are simultaneously represented by the modified representation method, which changes the reconstruction patch size of each facial area. Finally, the individualities of the eyes, nose, and mouth are retained by Maejima et al.'s approach. Our main contributions are as follows:

- Based on medical knowledge (Piérard et al., 2003), we synthesize an aged facial image containing aged wrinkles that are unique to the input image. To achieve this, we prepare a neutral facial image and multiple expression facial images and estimate the shapes and positions of future wrinkles from the expression facial images.
- We create a new aging database that is standardized for lighting, head pose, resolution, and race with only Japanese. This database will be made publicly available.

- We simultaneously synthesize aged wrinkles and other global aging textures by dividing the facial region into expression wrinkles and other areas. While Maejima et al. assumed constant patch sizes, we allow variable patch sizes for each facial area.

3 MEDICAL FACTS AND INPUT PREPARATION

Aging-induced changes in facial appearance have been widely researched in the medical field. Aging features have been classified into two types: surface skin changes such as spots, somberness, and wrinkles (Farage et al., 2008) and facial shape changes caused by sagging or gravity (Coleman and Grover, 2006). Consequently, the facial appearance of an individual changes greatly over time. Among the most significant features are facial wrinkles, which occur over the entire face. On account of their distinctive nature and wide distribution, wrinkles are used in person verification (Batool et al., 2013). Piérard et al. (Piérard et al., 2003) reported that expression changes cause wrinkles by repeatedly contracting the facial muscles in the same positions, destroying the rigid structure of the subcutaneous connective tissue. Therefore, expression wrinkles can be a powerful and effective metric for estimating the shapes and positions of the future wrinkles.

In our study, we estimate the shapes and positions of aged wrinkles from not only a neutral facial image but also multiple expression facial images with expression wrinkles. The input facial images are assumed to be nearly frontal and not occluded. In addition, as the shapes and positions of expression wrinkles are independent of expression categories, we prepare arbitrary single or multiple expression facial images. Since we focus on generating aged facial textures, sagging effect was not considered.

4 AGING DATABASE CONSTRUCTION

We first explain the processing of our aging database. Patch-based reconstruction by Visio-lization (Mohammed et al., 2009) requires a target age database representing wrinkles or the age-related features of skin textures. To prevent reconstruction failure, facial features such as eyes, nose, and mouth should be normalized at the same position in aging database. Therefore, we normalize the shapes and positions of the facial parts in our database by Maejima et al.'s approach (Maejima et al., 2014). In addition, we normalize the color in the aging database to that of the neutral facial images of the input person, as described by Kawai et al. (Kawai and Morishima, 2015). This step reduces the color differences between the database and the input.

5 EXPRESSION WRINKLES TRANSFER

This section describes the process of estimating the shapes and positions of aged wrinkles from facial images with neutral (Fig. 2(a)) and multiple expressions (Fig. 2(b)). The flow proceeds in three steps: expression normalization, expression wrinkles detection, and expression wrinkles transfer.

5.1 Expression Normalization

In Section 3, we mentioned that expression wrinkles in an expression facial image can effectively indicate the appearance of aged wrinkles in individuals. Therefore, we propose a method that estimates the shapes and positions of aged wrinkles by transferring expression wrinkles to a neutral facial image. To accomplish this properly, we take the correspondence between the neutral and expression facial shapes. First, the facial feature points are obtained from both images. The correspondence is then calculated by fitting the 2D facial template model into the neutral and expression facial images by Noh et al.'s (Noh et al., 2000) method, which smoothly interpolates between the known facial feature points (RBF centers) by RBF interpolation. Based on the fitted models, we reshape the expression facial images to the neutral facial shape by mesh deformation and generate expression normalized facial images (Fig. 2(c)).

5.2 Detection of Expression Wrinkles

To transfer the normalized expression wrinkles to the neutral facial image, we detect wrinkles by a simple automatic approach. The expression normalized facial images are processed by adaptive binary thresholding. Eight neighbors in a continuous area of the binary image are then labeled with the same index, and bounding boxes (blobs) are output for each labeled area. The number of significantly large areas is reduced by the facial feature points and the number of significantly small areas is reduced by setting a threshold number of pixels S (In this paper, we set $S = 1.5e+02$ when a facial area is about 1000×1000

(a) (b) (c) (d) (e)

Figure 2: Input facial images and transfer of expression wrinkles. (a) and (b) are neutral and expression facial images with expression wrinkles, respectively. (c) Expression facial images normalized to the neutral shape of facial images. (d) Wrinkles detected images. (e) Wrinkles estimated image, which is generated by transferring the expression wrinkles from (c) to (a).

pixels). The wrinkles are detected by an evaluation function that depends on the square closeness of the blobs and the density of the pixels:

$$\phi = \alpha\{1.0 - |\frac{4}{\pi}(tan^{-1}(\frac{h}{w}) - \frac{\pi}{4})|\} + (1-\alpha)\frac{s}{wh} \quad (1)$$

where α is a constant weight coefficient ($0 \leq \alpha \leq 1$), w and h are the width and height of the blobs, respectively, and s is the number of pixels. The first term describes the diagonal angle of the blobs from the horizontal line. As this angle approaches $\pi/4$, the blob more closely resembles a square and the first term in Eq. (1) increases. The second term describes the pixel density in a blob, and is greater when the pixel density is higher. Experimentally, we determine $\alpha = 0.5$ for $\phi < 0.8$. To reduce the detection of such blobs that are not wrinkles, we validate the wrinkles by reference to facial areas. From experiments, the blobs are reduced by using aspect ratio thresholding $h/w > 1.5$ around the eyes and $w/h > 1.5$ around the mouth. Fig. 2(d) shows the final detected results.

5.3 Transfer of Expression Wrinkles

The detected wrinkles are transferred to the neutral facial image, generating the aged wrinkles estimation result. We apply a seamless blending called Poisson image editing (Pérez et al., 2003). This method preserves the color of the target images by transferring the luminance gradient of the source image, thereby generating a synthesized image. The transfer requires a source image, a target image, and a mask image which determines the area to be synthesized. In our case, the source, target, and mask images Fig. 2(c), Fig. 2(a), and Fig. 2(d), respectively. Here, we pass the mask image through a dilation filter. A result (wrinkles estimated image) is shown in Fig. 2(e). Any existing wrinkle area in the neutral facial image is removed from the wrinkle transfer by applying the same wrinkle detection to the neutral facial image.

6 AGED FACE SYNTHESIS

6.1 Patch Sizes and Reconstructed Results Change

When reconstructing an image using the aging database, the reconstruction results appearance depends on the patch size, as indicated in Fig. 3. From Fig. 3(b) and (c), it can be seen that the large patch size reconstruction better represents the features of the target age, such as wrinkles and somberness, whereas the small patch size reconstruction better preserves the facial features of the input image, respectively. To retain the shapes and positions of the wrinkles estimated image, we apply small-patch reconstruction to the wrinkle-transferred regions. For other regions, we apply large-patch reconstruction to represent the entire facial features of the target age.

6.2 Patch-based Reconstruction using the Aging Database

Wrinkles estimated image is subjected to patch-based reconstruction. First, the wrinkles estimated image is normalized to the average facial shape in the same way as described for the aging database construction in Section 4. The division of areas into expression-wrinkle and non-expression-wrinkle areas is demonstrated in Fig. 4. Areas containing expression wrinkles are determined by referencing the wrinkles detected images (Fig. 2(d)). If the neutral facial image contains any aged wrinkles, its wrinkles detected image is also used in the area selection. Unlike Maejima et al. (Maejima et al., 2014), patch overlapping is not conducted, in order to better represent spots and somberness features. Also, patch continuity is disregarded to select a proper patch which relies only on luminance similarity between the aging database and the target image.

The small patches are reconstructed by selecting patches with the following evaluation function. Let I be the normalized wrinkles estimated image and D^n be the n-th facial image in the target age database. The

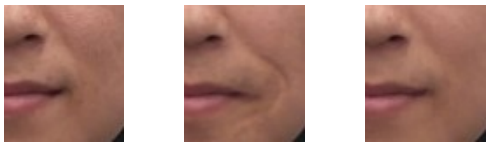

(a) (b) (c)

Figure 3: Effect of patch size on facial appearance. (a) Input image, (b) image reconstructed with large patches, and (c) image reconstructed with small patches. The large and small patches represent the databases features and the input image features, respectively.

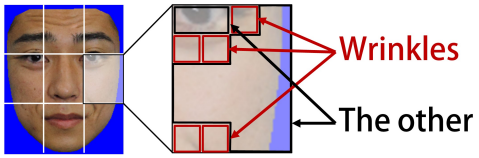

Figure 4: Assignment of expression wrinkles and other regions. The existing area containing wrinkles is reconstructed by small patches, and other areas are reconstructed by a single large patch.

evaluation function selects the patch with the smallest RGB Euclidean distance.

$$E_{wrinkle}(n) = \sum_{(x,y)\in P} ||I_{patch}(x,y) - D^n_{patch}(x,y)||^2 \quad (2)$$

where $I_{patch}(x,y)$ and $D^n_{patch}(x,y)$ are the RGB luminance vector (R,G,B) of the pixel (x,y) in a given patch and P denotes the entire area of the small patch. This evaluation function selects the patch that best matches the color of the corresponding patch on the input person. To more correctly estimate the shapes and positions of the expression wrinkles, we apply patch selection not only to the corresponding patch but also to neighboring patches that are concentrically shifted within a constant range. Non-expression-wrinkle patches are reconstructed by selecting patches with the smallest energy, as calculated by following Eq. (3).

$$E = \beta * E_{RGB}(n) + (1-\beta) * E_{HOG}(n) \quad (3)$$

where β is a constant weight coefficient selected from $[0,1]$. E_{RGB} and E_{HOG} are respectively defined by

$$E_{RGB}(n) = \sum_{(x,y)\in P^*} ||I_{patch}(x,y) - D^n_{patch}(x,y)||^2 \quad (4)$$

$$E_{HOG}(n) = ||HOG(I|P^*) - HOG(D^n|P^*)||^2 \quad (5)$$

where P^* denotes the entire region of non-expression wrinkles in the large patch. Eq. (4) and (5) are expressed in terms of the RGB Euclidean distance and HOG features (Dalal and Triggs, 2005), respectively.

(a) (b) (c)

Figure 5: Patch-based reconstruction and the synthesized result. (a) Reconstructed result. (b) Mask area excluding the eyes, nose, and mouth. (c) Result of synthesizing (a) to the normalized neutral facial image.

These equations incorporate the color of the input person into the reconstruction. With HOG features, we can select patches with spots, somberness and skin luster, which would better represent the target age features. Here, we set $\beta = 0.5$. The reconstructed result is shown in Fig. 5(a).

6.3 Synthesizing the Reconstructed Result

The reconstructed result should not be taken as the final aged facial image for two reasons. First, the boundary lines between patches are unnatural. Second, the reconstructed result loses the individuality of the input person's eyes, nose, and mouth. Hence, we adopt Maejima et al.'s approach (Maejima et al., 2014) and synthesize the reconstructed result to the neutral facial image. The synthesis is detailed in Maejima et al.'s paper (Maejima et al., 2014). The synthesized result is then reshaped to the neutral facial image with background, generating the final result (Fig. 5(c)).

7 EXPERIMENT AND EVALUATION

7.1 Synthesized Results

Fig. 6 shows facial images of a male in his 20s, and projected to ages of 50s to 70s by our method and Maejima et al.'s (Maejima et al., 2014) method. To compare results wrinkles position, we also present an image where the regions containing expression wrinkles were marked by hand on a neutral expression. Fig. 7 shows the facial images of the young male in his 20s projected to ages of 50s by our method and Maejima et al.'s (Maejima et al., 2014) method. For comparison, we also present the actual photographs of the young man at the target age (the ground truth). This aged facial image generated by our method considers the expression wrinkles which are only con-

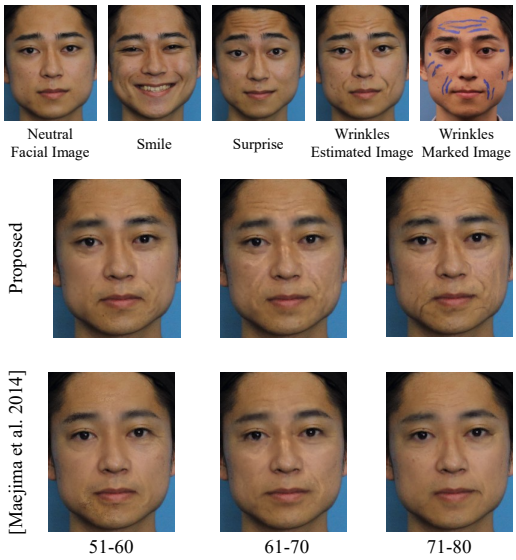

Figure 6: Results of $21-30$ year-old male, aged by the proposed method and [Maejima et al. 2014] method.

fined to the right side. As examples, we applied smile and surprise expressions in Fig. 6, and smile expressions in Fig. 7. The resolution of the normalized facial image is 300×300 pixels. In Maejima et al.'s method, the patch size was 40×40 pixels with an overlap of 20 pixels. In our method, the large and small patch sizes were 75×75 pixels and 5×5 pixels respectively and the small patches were shifted over concentric regions extending to 80 pixels. In both methods, these parameters were determined empirically. The numbers of pictures in each age group and gender of the aging database are listed in Table 1.

Comparing the results of the proposed and Maejima et al.'s method (Maejima et al., 2014) with the wrinkle-marked image in Fig. 6, we observe that the proposed method better represents the shapes and positions of the wrinkles; for example, the nasolabial folds and wrinkles in the forehead. Moreover, as demonstrated in Fig. 7, the nasolabial folds and wrinkles around the eyes are closer to the ground truth in our method than in Maejima et al.'s method. As mentioned in Piérard et al. (Piérard et al., 2003), our method preserves the individual qualities of the aged wrinkles. Moreover, these results imply that the spots and somberness in the non-expression-wrinkle area are better represented by our method than by Maejima et al. We attribute this success to the avoidance of overlapping and continuity, which suppress smoothing and propagate patches without aging features through the reconstruction step.

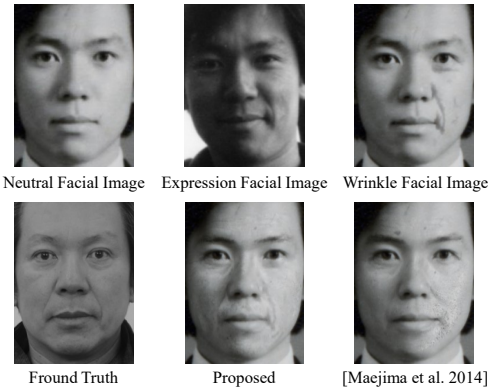

Figure 7: Results of aging a $21-30$ year old male to $51-60$ by our method and [Maejima et al. 2014] method.

7.2 Subjective Evaluation

To validate our method in terms of wrinkles individuality, synthesis naturalness, and how much it resembles the target age, we carried out the following subjective evaluation. By internet searching, we first selected neutral and expression facial images of 15 people aged in their 20s (11 males, 4 females), and ground truth images of the same people at a later age. In 2, 9 and 4 of the ground truth images, the subjects were aged in their 50s, 60s, and 70s, respectively. When the expression wrinkles of an input person were too poorly resolved to detect, the wrinkles were manually selected in the mask image. The 15 internet subjects were also chosen because their ground truth images exhibit noticeably aged features such as wrinkles and old skin textures. The images were presented to 32 study participants (21 males, 11 females). Specifically, an image created by our proposed method and Maejima et al.'s (Maejima et al., 2014) method were randomly placed at either side of the ground truth, and referred to as facial image A and facial image B, respectively. A neutral facial image of the same target person at a younger age was also presented. The 32 participants reported their answers on a questionnaire. To ensure that answers are focused on the unique aging process of the target person, and not the maturity of the person's appearance, we provided the actual ages below the neutral facial image and the ground truth. To emphasize that the target age equals the ground truth age, we also wrote the age below facial image *A* and facial image *B*. The participants evaluated the naturalness of facial images *A* and *B* on a 5-point Likert scale. They were asked to estimate the ages of images A and B in decade units (20s to 70s). Also, they were asked which image they perceived to best match the ground truth in terms of the wrinkles individuality, the age-likeness of the aged wrinkles, and the age-likeness of other skin textures

Table 1: Number of pictures stored for each age group and gender.

Age range	Male	Female	Subtotal
21-30	14	27	41
31-40	22	31	53
41-50	36	71	107
51-60	7	9	16
61-70	10	10	20
71-80	9	5	14
Total	98	153	251

Table 2: Evaluation items in the subjective evaluation.

Likert scale	Synthesis naturalness	Comparison between the ground truth
1	Disagree	A is closer
2	Slightly disagree	A is slightly closer
3	Neither agree nor disagree	Neither A nor B is closer
4	Slightly agree	B is slightly closer
5	Agree	B is closer

on a 5-point Likert scale. The options for evaluating naturalness are given in Table 2. Wrinkles individuality refers to how accurately the shapes and positions of the wrinkles match those of the ground truth. Age-likeness of the aged wrinkles (and skin textures) refers to whether the appearances of the aged wrinkles (and skin textures other than wrinkles) are consistent with the processed image and the ground truth. Fig. 8 presents the average scores of the 32 participants for each target person (labeled by their ID) assigned to individuality and age-likeness of the aged wrinkles and the age-likeness of other skin textures. Scores of 5, 3 and 1 mean that our method is decidedly closer to the ground truth, no closer than, and decidedly further from the ground truth, respectively, than Maejima's method. Table 3 gives the average scores and standard deviations (SD) of the 15 image sets evaluated by the 32 participants. The aging error was computed as the ground truth age minus the perceived age. Table 3 also lists the average naturalness scores and their standard deviations rated (SD) by the 32 participants.

As shown in Fig. 8 our method was rated higher than 3.0 in every item for every target person. The total average scores and their standard deviations were 4.00 ± 0.978 for wrinkles individuality, 4.29 ± 0.836 for age-likeness of aged wrinkles, and 3.93 ± 0.975 for age-likeness of other skin textures. Although the scores are slightly variable, our method clearly outperformed the previous method in all three evaluation terms, confirming that our method better represents that wrinkles individuality and surface skin appearance of the ground truth than the previous method.

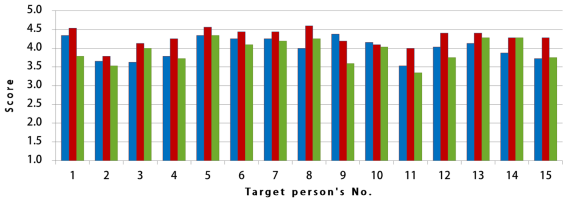

Figure 8: Evaluation scores of wrinkle individuality (blue bars), age-likeness of the wrinkles (red bars), and age-likeness of the skin textures (green bars).

Table 3: Statistics of synthesized image quality and age error.

	Aging Error	Synthesis Naturalness
	Average $\pm$ *SD*	*Average* $\pm$ *SD*
Proposed	13.4 ± 7.60	3.41 ± 1.22
Maejima et al.	25.4 ± 7.23	3.91 ± 1.06

To investigate how closely the appearance of the entire skin texture approaches that of the ground truth, we asked participants to assess the ages of our generated images. As the age of each image was provided, and the experimental environment was designed so that participants would focus solely on the aging process of the targets, the validity of an aged facial image could be effectively estimated by the above-defined aging error.

Table 3 reveals that the aging error is lower in our method than in the previous method, indicating that the aged facial image generated by our method better resembles the ground truth. As for the synthesis naturalness, both methods scored above 3.0, although the previous method was rated higher than ours. The naturalness of our method may have been reduced by the inconsistency of the wrinkle textures across the entire face.

7.3 Limitations

Several problems and tasks are currently unresolved in our method. Wrinkle detection might be improved by Batool et al.'s (Batool and Chellappa, 2012) method, and facial sagging could be properly added by Kemelmacher et al.'s (Kemelmacher-Shlizerman et al., 2014) method. Induced by the recent successes on image generation based on Generative Adversarial Network (Liao et al., 2017), applying such methods would help generating high-quality and more accurate images. Still, our observation of estimating the wrinkle position from the expression images would certainly be the important asset to improve the accuracy of the generated wrinkles appearances and positions.

8 CONCLUSION

The medical literature reports that aged wrinkles are the permanent impressions of expression wrinkles. Based on this knowledge, we proposed a method that captures the individuality of a person's aging-induced wrinkles. From subject evaluations it is confirmed that preserving the wrinkles individuality effectively improves the visual plausibility. We aim to examine our ideas with image generation approaches based on Generative Adversarial Network (Liao et al., 2017) to further improve our results.

Proposed method has a wide scalability in 3DCG facial animations. In recent years, there are several methods dealing with aged faces in 3DCG field such as high fidelity 3D facial shape reconstruction (Cao et al., 2015), and aged textures' optical property modeling and rendering (Iglesias-Guitian et al., 2015). These methods are focusing on accurately reconstructing or rendering the aged faces in real time. Our method can provide high resolution aged facial textures which considers both the facial and wrinkles individuality. This enables making 3DCG aged facial animation with better quality. Thus, we aim to realize such system by improving our method in terms of 3DCG facial animation in the future.

ACKNOWLEDGEMENT

This work was supported by JST ACCEL Grant Number JPMJAC1602, Japan.

REFERENCES

(2011). Age progression, forensic and medical artist. https://aurioleprince.wordpress.com/.

Batool, N. and Chellappa, R. (2012). Modeling and detection of wrinkles in aging human faces using marked point processes. In *European Conference on Computer Vision*, pages 178–188. Springer.

Batool, N., Taheri, S., and Chellappa, R. (2013). Assessment of facial wrinkles as a soft biometrics. In *2013 10th IEEE International Conference and Workshops on Automatic Face and Gesture Recognition (FG)*, pages 1–7. IEEE.

Cao, C., Bradley, D., Zhou, K., and Beeler, T. (2015). Real-time high-fidelity facial performance capture. *ACM Transactions on Graphics (TOG)*, 34(4):46.

Coleman, S. R. and Grover, R. (2006). The anatomy of the aging face: volume loss and changes in 3-dimensional topography. *Aesthetic Surgery Journal*, 26(1 Supplement):S4–S9.

Dalal, N. and Triggs, B. (2005). Histograms of oriented gradients for human detection. In *IEEE Computer Society Conference on Computer Vision and Pattern Recognition, 2005*, volume 1, pages 886–893. IEEE.

Farage, M., Miller, K., Elsner, P., and Maibach, H. (2008). Intrinsic and extrinsic factors in skin ageing: a review. *International Journal of Cosmetic Science*, 30(2):87–95.

Iglesias-Guitian, J. A., Aliaga, C., Jarabo, A., and Gutierrez, D. (2015). A biophysically-based model of the optical properties of skin aging. *Computer Graphics Forum*, 34(2):45–55.

Kawai, M. and Morishima, S. (2015). Focusing patch: Automatic photorealistic deblurring for facial images by patch-based color transfer. In *Proceedings of International Conference on Multimedia Modeling*, pages 155–166. Springer.

Kemelmacher-Shlizerman, I., Suwajanakorn, S., and Seitz, S. M. (2014). Illumination-aware age progression. In *Proceedings of the IEEE Conference on Computer Vision and Pattern Recognition*, pages 3334–3341.

Liao, J., Yao, Y., Yuan, L., Hua, G., and Kang, S. B. (2017). Visual attribute transfer through deep image analogy. *arXiv preprint arXiv:1705.01088v2*.

Maejima, A., Mizokawa, A., Kuwahara, D., and Morishima, S. (2014). Facial aging simulation by patch-based texture synthesis with statistical wrinkle aging pattern model. In *Mathematical Progress in Expressive Image Synthesis I*, pages 161–170. Springer.

Mohammed, U., Prince, S. J., and Kautz, J. (2009). Visiolization: generating novel facial images. In *ACM Transactions on Graphics (TOG)*, volume 28, page 57. ACM.

Noh, J.-y., Fidaleo, D., and Neumann, U. (2000). Animated deformations with radial basis functions. In *Proceedings of the ACM symposium on Virtual reality software and technology*, pages 166–174. ACM.

Park, U., Tong, Y., and Jain, A. K. (2010). Age-invariant face recognition. *IEEE Transactions on Pattern Analysis and Machine Intelligence*, 32(5):947–954.

Patterson, E., Ricanek, K., Albert, M., and Boone, E. (2006). Automatic representation of adult aging in facial images. In *Proc. IASTED International Conference on Visualization, Imaging, and Image Processing*, pages 171–176.

Pérez, P., Gangnet, M., and Blake, A. (2003). Poisson image editing. In *ACM Transactions on Graphics (TOG)*, volume 22, pages 313–318. ACM.

Piérard, G. E., Uhoda, I., and Piérard-Franchimont, C. (2003). From skin microrelief to wrinkles. an area ripe for investigation. *Journal of Cosmetic Dermatology*, 2(1):21–28.

Scherbaum, K., Sunkel, M., Seidel, H.-P., and Blanz, V. (2007). Prediction of individual non-linear aging trajectories of faces. In *Computer Graphics Forum*, volume 26, pages 285–294. Wiley Online Library.

Shu, X., Tang, J., Lai, H., Liu, L., and Yan, S. (2015). Personalized age progression with aging dictionary. In *Proceedings of the IEEE International Conference on Computer Vision*, pages 3970–3978.

Shu, X., Xie, G.-S., Li, Z., and Tang, J. (2016). Age pro-

gression: current technologies and applications. *Neurocomputing*, 208:249–261.

Suo, J., Zhu, S.-C., Shan, S., and Chen, X. (2010). A compositional and dynamic model for face aging. *IEEE Transactions on Pattern Analysis and Machine Intelligence*, 32(3):385–401.

Wang, W., Cui, Z., Yan, Y., Feng, J., Yan, S., Shu, X., and Sebe, N. (2016). Recurrent face aging. In *Proceedings of the IEEE Conference on Computer Vision and Pattern Recognition*, pages 2378–2386.

Yang, H., Huang, D., Wang, Y., Wang, H., and Tang, Y. (2016). Face aging effect simulation using hidden factor analysis joint sparse representation. *IEEE Transactions on Image Processing*, 25(6):2493–2507.

Zhang, Z., Song, Y., and Qi, H. (2017). Age progression/regression by conditional adversarial autoencoder. *arXiv preprint arXiv:1702.08423*.